ATLAS NOTE

ATL-PHYS-PUB-2015-030

27th July 2015

First validation plots in preparation for a search for new phenomena in final states with large jet multiplicities and missing transverse momentum at $\sqrt{s} = 13$ TeV proton–proton collisions using the ATLAS experiment

The ATLAS Collaboration

Abstract

A first implementation of the data-driven QCD background estimate for the ATLAS SUSY 'Multijet' search is performed on 72 pb^{-1} of early 2015 $\sqrt{s} = 13$ TeV proton–proton collision data. The method from previous searches in Run-1 is shown to still be effective.

1 Introduction

Supersymmetry (SUSY) [1–9] is a theoretically favoured extension of the Standard Model (SM), which for each degree of freedom of the SM predicts another degree of freedom with a different spin. These degrees of freedom combine into physical superpartners of the SM particles: scalar partners of quarks and leptons (squarks ($\tilde{q}$) and sleptons ($\tilde{\ell}$)), fermionic partners of gauge and Higgs bosons (gluinos ($\tilde{g}$), charginos ($\tilde{\chi}_i^{\pm}$, with i = 1,2) and neutralinos ($\tilde{\chi}_i^0$ with i = 1,2,3,4)), all with identical quantum number to their SM partners, except spin. Since no superpartner of any of the SM particles has been observed, SUSY must be a broken symmetry, with a mechanism for breaking the symmetry being at some higher energy scale.

The discovery (or exclusion) of weak-scale SUSY is one of the highest physics priorities for the LHC. The primary target for early supersymmetry searches at the proton–proton (pp) collisions at centre-of-mass energies of 13 TeV of the LHC, given their large expected cross-section, are the production of gluinos, and first and second generation squarks. Under the hypothesis of R-parity conservation [10–13], SUSY partners are produced in pairs and decay to the Lightest Supersymmetric Particle (LSP) which is stable and in a large variety of models is assumed to be the lightest neutralino ($\tilde{\chi}_1^0$) that escapes detection.

The undetected $\tilde{\chi}_1^0$ would result in substantial missing transverse momentum ($\vec{E}_{\mathrm{T}}^{\mathrm{miss}}$), while the rest of the cascade, originating from the decays of squarks and gluinos, would yield final states with multiple jets and possibly leptons.

This note describes the first results related to the update of a series of previously reported searches for new particles [14–17] in multijet+$E_{\mathrm{T}}^{\mathrm{miss}}$ final states. The most recent of those analyses was detailed in a summer 2013 paper [17] based on data from the full Run-1 $\sqrt{s}$ = 8 TeV dataset, corresponding to an integrated luminosity of 20.3 fb^{-1}.

The search channel is defined by the characteristic of looking for supersymmetric models which exhibit longer decay chains such that the signature is of large jet multiplicity and $E_{\mathrm{T}}^{\mathrm{miss}}$. In contrast to other strong production searches here we concentrate on decays with low levels of $E_{\mathrm{T}}^{\mathrm{miss}}$ and do not use this as a major discriminant against $t\bar{t}$, W+jets and Z+jets backgrounds. As a consequence, the dominant background to the search is Standard Model multijet events (denoted 'QCD' in the following). The processes leading to high jet multiplicities in these events are such that a data-driven estimate yields a more precise background prediction than one based on Monte Carlo (MC) simulation of these QCD processes. This note describes and demonstrates a first implementation of this background estimate in very early Run-2 data.

2 Dataset, Triggers, Event Selection and Simulation

2.1 Dataset and Trigger

The dataset used for this note was collected by the ATLAS detector in proton–proton collisions at the LHC with a bunch spacing of 50ns and at a centre-of-mass energy $\sqrt{s}$ = 13 TeV, from 6$^{\mathrm{th}}$ to 17$^{\mathrm{th}}$ July 2015. After applying beam-, data- and detector-quality criteria, the total available integrated luminosity is 72 pb^{-1}. It is derived, following a methodology similar to that detailed in Ref. [18], from a preliminary calibration of the luminosity scale using a pair of x-y beam-separation scans performed in June 2015. The uncertainty on the integrated luminosity is ± 9%.

The data were selected with a two-level trigger system that required 4 jets with $p_{\mathrm{T}} > 15$ GeV at the hardware level. At the software level, 5-jet and $\geq$ 6-jet events were selected with a trigger that required ≥ 5 and ≥ 6 jets respectively with $p_{\mathrm{T}} > 45$ GeV. For this data-taking period, the 5-jet trigger was accepting only every 6$^{\mathrm{th}}$ event due to bandwidth considerations, resulting in an integrated luminosity of 12 pb^{-1} for 5-jet events. The 6-jet trigger was unaffected by such considerations, so 6-jet and higher multiplicity events have the full integrated luminosity of 72 pb^{-1} available.

2.2 Object Definition and Event Selection

Jets are reconstructed using the anti-k_t clustering algorithm [19, 20] and jet radius parameter $R = 0.4$. Events with 'bad' jets (originating from cosmic rays, beam background and detector noise) are vetoed, as are events with isolated leptons (e, μ) with p_{T} above 10 GeV. Following this, only well-measured and isolated jets (as described in Ref. [21]), within $|\eta| < 2.0$ and with $p_{\mathrm{T}} > 50$, are considered - with the additional constraint that they have a fraction of track p_{T} matched to the primary vertex, JVF, > 0.25 in order to reduce the effect of pileup. The regions of interest are then defined by the number of such jets (5, 6 or 7). Jets with a looser definition, required to have $p_{\mathrm{T}} > 40$ GeV, $|\eta| < 2.8$ and the same JVF requirement as above, are used to construct the variable $H_{\mathrm{T}} = \sum_i p_{\mathrm{T}}^{\mathrm{jet}\ i}$. This is used in the construction of the discriminant $E_{\mathrm{T}}^{\mathrm{miss}}/\sqrt{H_{\mathrm{T}}}$ - a proxy for the $E_{\mathrm{T}}^{\mathrm{miss}}$ significance. The calculation of the missing transverse momentum, $E_{\mathrm{T}}^{\mathrm{miss}}$, is based on the vector sum of the calibrated p_{T} of reconstructed jets (with $p_{\mathrm{T}} > 20$ GeV and $|\eta| < 4.5$), electrons, muons and photons and the inner-detector tracks not belonging to these reconstructed objects - as described in Ref. [22].

Additionally to the Run-1 cuts a lower limit is placed on H_{T} of 600 GeV to simplify the multi-jet background estimation procedure, and while in Run-1 additional requirements were placed on b-jet multiplicity, here no such requirements have been applied to increase statistics.

2.3 MC Background Estimation

In order to estimate the QCD background from the data, the contribution from other ('leptonic') backgrounds must be subtracted. The Monte Carlo samples were generated with an expected pileup (mean number of interactions per bunch crossing) distribution, and they have been re-weighted so that the mean pileup distribution matches the observed distribution in the data. The MC samples used are as follows.

For the generation of $t\bar{t}$ and single top-quarks in the Wt and s-channels the `PowHeg-Box` v2 [23] generator with the CT10 PDF sets in the matrix element calculations is used. Electroweak t-channel single top-quark events are generated using the `PowHeg-Box` v1 generator. This generator uses the 4-flavour scheme for the NLO matrix elements calculations together with the fixed four-flavour PDF set CT10f4. For this process, the top quarks are decayed using `MadSpin` [24] preserving all spin correlations, while for all processes the parton shower, fragmentation, and the underlying event are simulated using `PYTHIA` v6.428 [25] with the CTEQ6L1 PDF sets and the corresponding Perugia 2012 tune (P2012) [26]. The top mass is set to 172.5 GeV. The `EvtGen` v1.2.0 program [27] is used for properties of the bottom and charm hadron decays. The predicted $t\bar{t}$ production cross section is calculated to NNLO in perturbative QCD, including soft-gluon resummation to NNLL order (see [28] and references therein).

Events containing W bosons with associated jets are simulated using `MadGraph` v2.2.2 [29] at Leading Order interfaced to the `PYTHIA` 8.186 [25, 30] parton shower model. The A14 tune is used together with

the NNPDF2.3LO PDF set [31]. The EvtGen v1.2.0 program [27] is used for properties of the bottom and charm hadron decays. The W + jets events are normalised to NNLO cross sections.

Events containing Z bosons associated with jets are simulated using the SHERPA v2.1.1 [32] generator. Matrix elements are calculated for up to two partons at NLO and four partons at LO using the Comix [33] and OpenLoops [34] matrix element generators and merged with the SHERPA parton shower [35] using the ME+PS@NLO prescription [36]. The CT10 parton distribution functions (PDF) [37] is used in association to authors tuning. The Z + jets events are normalised to NNLO cross sections.

The benchmark signal model shown here is a 'two step' gluino decay model described in [17], i.e. $pp \to \tilde{g}\tilde{g}, \tilde{g} \to qq\tilde{\chi}_1^{\pm}, \tilde{\chi}_1^{\pm} \to W^{\pm}\tilde{\chi}_2^0, \tilde{\chi}_2^0 \to Z\tilde{\chi}_1^0$; defined by mass parameters $m_{\tilde{g}}$ and $m_{\tilde{\chi}_1^0}$, with $m_{\tilde{\chi}_1^{\pm}} = \frac{1}{2}(m_{\tilde{g}} + m_{\tilde{\chi}_1^0})$ and $m_{\tilde{\chi}_2^0} = \frac{1}{2}(m_{\tilde{\chi}_1^{\pm}} + m_{\tilde{\chi}_1^0})$. The signal events are simulated in the same way as those of W + jets, i.e. using MadGraph v2.2.2 at LO interfaced to PYTHIA 8.186, and are normalised to gluino production cross-sections calculated to NLO + NLL (see [38]).

3 QCD Multijet Background Estimation

A data-driven estimate of the QCD multijet background is required in regions with very high jet multiplicities and hence very low event counts. To obtain a good estimate of this background it is necessary to perform an extrapolation from low to high jet multiplicity. The principal discriminating variable in Run-1 was $E_{\mathrm{T}}^{\mathrm{miss}}/\sqrt{H_{\mathrm{T}}}$ (constructed as described in section 2.2), with the signal regions defined with $E_{\mathrm{T}}^{\mathrm{miss}}/\sqrt{H_{\mathrm{T}}} > 4\mathrm{GeV}^{1/2}$. The shape of $E_{\mathrm{T}}^{\mathrm{miss}}/\sqrt{H_{\mathrm{T}}}$ is largely independent of jet multiplicity (when jet multiplicity is sufficiently high) [17]. In Run-1 a re-weighting of this template based on the amount of low energy deposits in the calorimeter not clustered into jets was performed, however, due to the H_{T} cut applied here this complication is not necessary.

Following the event selection described in section 2.2, an $E_{\mathrm{T}}^{\mathrm{miss}}/\sqrt{H_{\mathrm{T}}}$ template is extracted from 5-jet events. This is done by subtracting the MC prediction of the leptonic backgrounds (normalised to predicted cross-sections, 72 pb^{-1} and trigger live fraction of $\sim 1/6$) from the data, as shown in figure 1. This shape is then applied to 6-jet (figure 2) data by adding it to the MC predictions in this region and normalising to data with $E_{\mathrm{T}}^{\mathrm{miss}}/\sqrt{H_{\mathrm{T}}} < 1.5\ \mathrm{GeV}^{1/2}$. The same procedure is performed for a 6-jet to 7-jet extrapolation, the result of which is shown in figure 3. In contrast to the $5 \to 6$ and $6 \to 7$ jets extrapolation shown here, the full Run-1 dataset search performed it from $6 \to 8, 9, \geq 10$ jets to reach these signal regions (which were defined with the one additional requirement of b-jet multiplicity slicing), which we do not show here because there is insufficient data for a higher multiplicity extrapolation. In both extrapolations performed here, good agreement is seen between the template and data within statistical uncertainty.

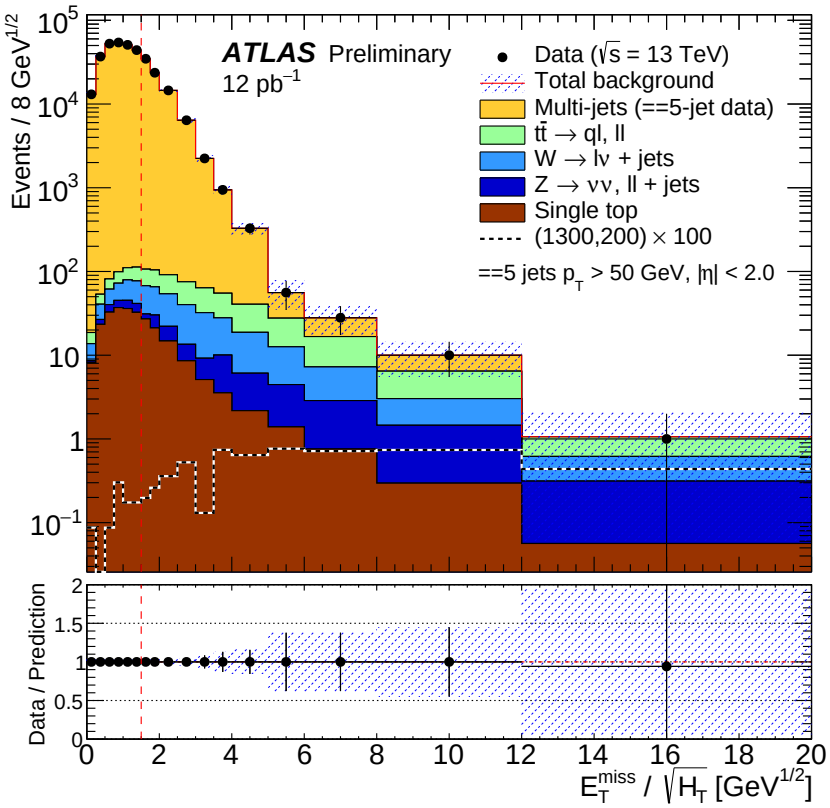

Figure 1: $E_{\mathrm{T}}^{\mathrm{miss}}/\sqrt{H_{\mathrm{T}}}$ template (exactly 5 jets) in orange, labelled 'Multi-jets', taken as the difference between data and the sum of expected 'leptonic' backgrounds. There are no data events in the overflow bins, i.e. with $E_{\mathrm{T}}^{\mathrm{miss}}/\sqrt{H_{\mathrm{T}}} > 20$ GeV$^{1/2}$. The blue hatched band shows the statistical uncertainty on the template. Systematic uncertainties are not evaluated, but are expected to be of a similar magnitude or smaller. The black dashed line shows the expectation for the 'two-step' signal point with $(m_{\tilde{g}}, m_{\tilde{\chi}_1^0}) = (1300, 200)$ GeV, scaled by a factor of 100. The vertical red dashed line demarks the normalisation region of $E_{\mathrm{T}}^{\mathrm{miss}}/\sqrt{H_{\mathrm{T}}} < 1.5$ GeV$^{1/2}$.

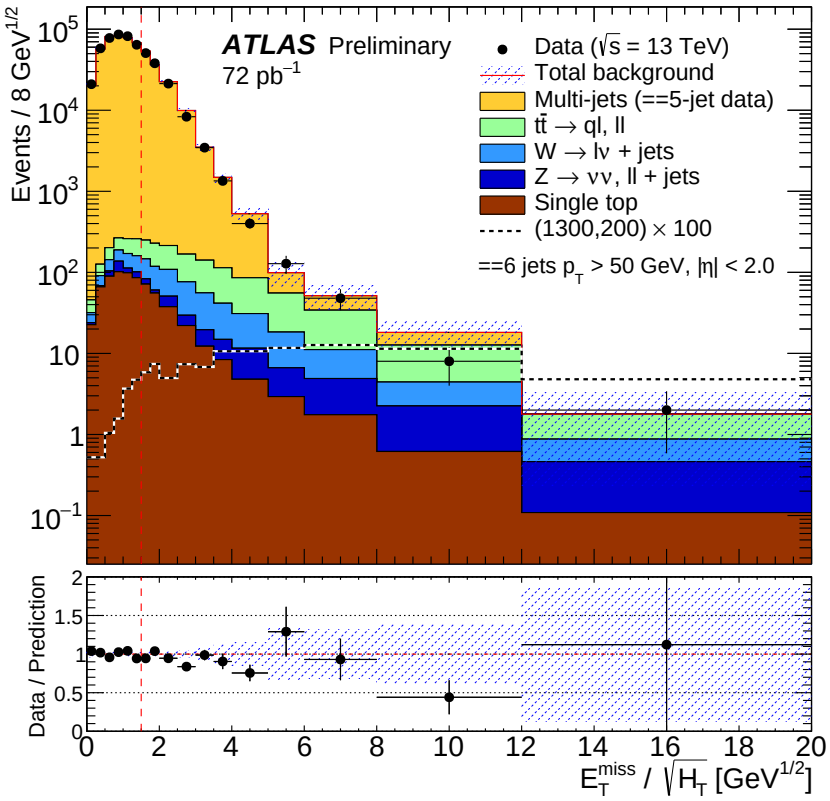

Figure 2: $E_{\mathrm{T}}^{\mathrm{miss}}/\sqrt{H_{\mathrm{T}}}$ template (exactly 5 jets) applied to data with exactly 6 jets. Template normalised to data with $E_{\mathrm{T}}^{\mathrm{miss}}/\sqrt{H_{\mathrm{T}}} < 1.5$ GeV$^{1/2}$. There are no data events in the overflow bins, i.e. with $E_{\mathrm{T}}^{\mathrm{miss}}/\sqrt{H_{\mathrm{T}}} > 20$ GeV$^{1/2}$. The blue hatched band shows the statistical uncertainty on the template. Systematic uncertainties are not evaluated, but are expected to be of a similar magnitude or smaller. The black dashed line shows the expectation for the 'two-step' signal point with $(m_{\tilde{g}}, m_{\tilde{\chi}_1^0}) = (1300, 200)$ GeV, scaled by a factor of 100. The vertical red dashed line demarks the normalisation region of $E_{\mathrm{T}}^{\mathrm{miss}}/\sqrt{H_{\mathrm{T}}} < 1.5$ GeV$^{1/2}$.

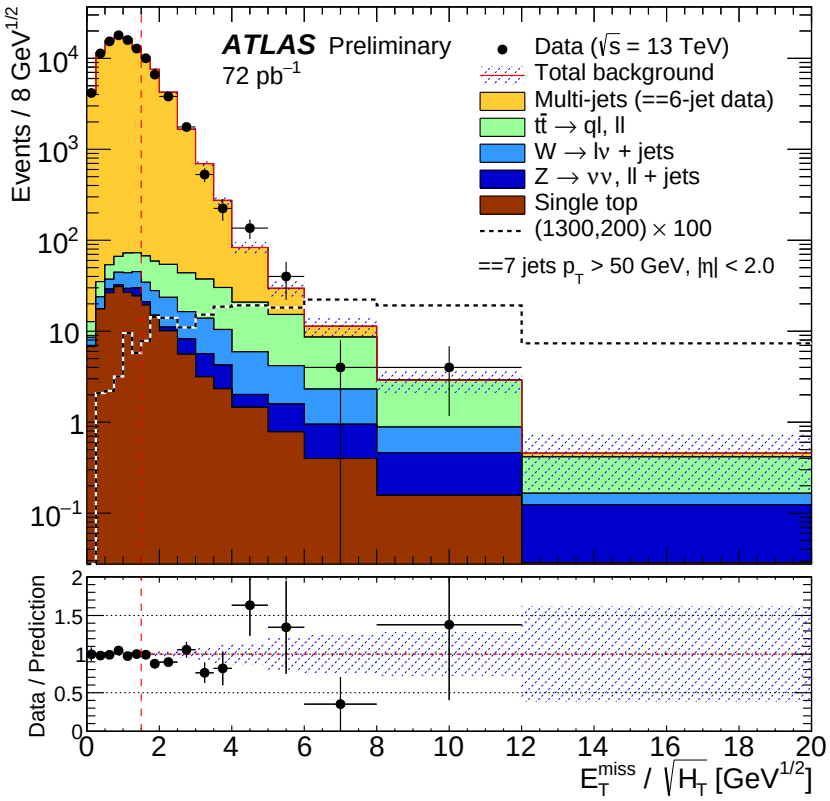

Figure 3: $E_{\mathrm{T}}^{\mathrm{miss}}/\sqrt{H_{\mathrm{T}}}$ template (exactly 6 jets) applied to data with exactly 7 jets. Template normalised to data with $E_{\mathrm{T}}^{\mathrm{miss}}/\sqrt{H_{\mathrm{T}}} < 1.5$ GeV$^{1/2}$. There are no data events in the overflow bins, i.e. with $E_{\mathrm{T}}^{\mathrm{miss}}/\sqrt{H_{\mathrm{T}}} > 20$ GeV$^{1/2}$. The blue hatched band shows the statistical uncertainty on the template. Systematic uncertainties are not evaluated, but are expected to be of a similar magnitude or smaller. The black dashed line shows the expectation for the 'two-step' signal point with $(m_{\tilde{g}}, m_{\tilde{\chi}_1^0}) = (1300, 200)$ GeV, scaled by a factor of 100. The vertical red dashed line demarks the normalisation region of $E_{\mathrm{T}}^{\mathrm{miss}}/\sqrt{H_{\mathrm{T}}} < 1.5$ GeV$^{1/2}$.

4 Conclusion

The technique used for the estimation of the principal background to the SUSY Multijet search in 2012 $\sqrt{s} = 8$ TeV data has been repeated in early 2015 $\sqrt{s} = 13$ TeV data. Good agreement is seen between the $E_{\mathrm{T}}^{\mathrm{miss}}/\sqrt{H_{\mathrm{T}}}$ template and data, building confidence that this method will be suitable for a similar search in Run-2.

References

[1] H. Miyazawa, *Baryon Number Changing Currents*, Prog. Theor. Phys. **36 (6)** (1966) 1266.

[2] P. Ramond, *Dual Theory for Free Fermions*, Phys. Rev. **D 3** (1971) 2415.

[3] Y. A. Golfand and E. P. Likhtman,
Extension of the Algebra of Poincare Group Generators and Violation of p Invariance,
JETP Lett. **13** (1971) 323, [Pisma Zh.Eksp.Teor.Fiz.13:452-455,1971].

[4] A. Neveu and J. H. Schwarz, *Factorizable dual model of pions*, Nucl. Phys. **B 31** (1971) 86.

[5] A. Neveu and J. H. Schwarz, *Quark Model of Dual Pions*, Phys. Rev. **D 4** (1971) 1109.

[6] J. Gervais and B. Sakita, *Field theory interpretation of supergauges in dual models*,
Nucl. Phys. **B 34** (1971) 632.

[7] D. V. Volkov and V. P. Akulov, *Is the Neutrino a Goldstone Particle?*,
Phys. Lett. **B 46** (1973) 109.

[8] J. Wess and B. Zumino, *A Lagrangian Model Invariant Under Supergauge Transformations*,
Phys. Lett. **B 49** (1974) 52.

[9] J. Wess and B. Zumino, *Supergauge Transformations in Four-Dimensions*,
Nucl. Phys. **B 70** (1974) 39.

[10] P. Fayet, *Supersymmetry and Weak, Electromagnetic and Strong Interactions*,
Phys.Lett. **B64** (1976) 159.

[11] P. Fayet, *Spontaneously Broken Supersymmetric Theories of Weak, Electromagnetic and Strong Interactions*, Phys.Lett. **B69** (1977) 489.

[12] G. R. Farrar and P. Fayet, *Phenomenology of the Production, Decay, and Detection of New Hadronic States Associated with Supersymmetry*, Phys.Lett. **B76** (1978) 575–579.

[13] P. Fayet, *Relations Between the Masses of the Superpartners of Leptons and Quarks, the Goldstino Couplings and the Neutral Currents*, Phys.Lett. **B84** (1979) 416.

[14] ATLAS Collaboration, *Search for new phenomena in final states with large jet multiplicities and missing transverse momentum using* $\sqrt{s}$ = 7 *TeV pp collisions with the ATLAS detector*,
JHEP **11** (2011) 099, arXiv: 1110.2299 [hep-ex].

[15] ATLAS Collaboration, *Hunt for new phenomena using large jet multiplicities and missing transverse momentum with ATLAS in* $4.7\,fb^{-1}$ *of* $\sqrt{s}$ = 7 *TeV proton-proton collisions*,
JHEP **1207** (2012) 167, arXiv: 1206.1760 [hep-ex].

[16] ATLAS Collaboration, *Search for new phenomena using large jet multiplicities and missing transverse momentum with ATLAS in 5.8* fb^{-1} *of* $\sqrt{s}$ = 8 *TeV proton-proton collisions*,
ATLAS-CONF-2012-103, ATLAS-COM-CONF-2012-142,
URL: https://cds.cern.ch/record/1472672.

[17] ATLAS Collaboration,
Search for new phenomena in final states with large jet multiplicities and missing transverse momentum at $\sqrt{s}$*=8 TeV proton-proton collisions using the ATLAS experiment*,
JHEP **1310** (2013) 130, arXiv: 1308.1841 [hep-ex].

[18] ATLAS Collaboration, *Improved luminosity determination in pp collisions at sqrt(s) = 7 TeV using the ATLAS detector at the LHC*, Eur.Phys.J. **C73**.8 (2013) 2518,
arXiv: 1302.4393 [hep-ex].

[19] M. Cacciari, G. P. Salam and G. Soyez, *The anti-k_t jet clustering algorithm*, JHEP **04** (2008) 063, arXiv: 0802.1189.

[20] M. Cacciari and G. P. Salam, *Dispelling the N^3 myth for the k_t jet-finder*, Phys. Lett. **B641** (2006) 57–61, arXiv: hep-ph/0512210.

[21] ATLAS Collaboration, *Selection of jets produced in proton-proton collisions with the ATLAS detector using 2015 data*, ATL-PHYS-PUB-2015-023 (2015).

[22] ATLAS Collaboration, *Expected performance of missing transverse momentum reconstruction for the ATLAS detector at $\sqrt{s}$ = 13 TeV*, ATLAS-CONF-2015-029 (2015).

[23] S. Alioli et al., *A general framework for implementing NLO calculations in shower Monte Carlo programs: the POWHEG BOX*, JHEP **1006** (2010) 043, arXiv: 1002.2581 [hep-ph].

[24] P. Artoisenet et al., *Automatic spin-entangled decays of heavy resonances in Monte Carlo simulations*, JHEP **1303** (2013) 015, arXiv: 1212.3460 [hep-ph].

[25] T. Sjöstrand, S. Mrenna and P. Z. Skands, *PYTHIA 6.4 physics and manual*, JHEP **05** (2006) 026, arXiv: hep-ph/0603175.

[26] P. Z. Skands, *Tuning Monte Carlo Generators: The Perugia Tunes*, *Phys. Rev.* **D 82** (2010) 074018, arXiv: 1005.3457 [hep-ph].

[27] D. J. Lange, *The EvtGen particle decay simulation package*, Nucl. Instrum. Meth. **A462** (2001) 152.

[28] M. Czakon and A. Mitov, *Top++: a program for the calculation of the top-pair cross-section at hadron colliders*, Computer Physics Communications **185** (2014) 2930, arXiv: 1112.5675 [hep-ph].

[29] J. Alwall et al., *The automated computation of tree-level and next-to-leading order differential cross sections, and their matching to parton shower simulations*, JHEP **2014** (2014) 158, arXiv: 1405.0301 [hep-ph].

[30] T. Sjöstrand, S. Mrenna and P. Z. Skands, *A Brief Introduction to PYTHIA 8.1*, Comput.Phys.Commun. **178** (2008) 852–867, arXiv: 0710.3820 [hep-ph].

[31] R. Ball et al., *Parton distributions with LHC data*, Nucl. Phys. **B 867** (2013) 244–289, arXiv: 1207.1303 [hep-ph].

[32] T. Gleisberg et al., *Event generation with SHERPA 1.1*, JHEP **0902** (2009) 007, arXiv: 0811.4622 [hep-ph].

[33] T. Gleisberg and S. Hoche, *Comix, a new matrix element generator*, JHEP **0812** (2008) 039, arXiv: 0808.3674 [hep-ph].

[34] F. Cascioli, P. Maierhofer and S. Pozzorini, *Scattering Amplitudes with Open Loops*, Phys. Rev. Lett. **108** (2012) 111601, arXiv: 1111.5206 [hep-ph].

[35] S. Schumann and F. Krauss, *A Parton shower algorithm based on Catani-Seymour dipole factorisation*, JHEP **0803** (2008) 038, arXiv: 0709.1027 [hep-ph].

[36] S. Hoeche et al., *QCD matrix elements + parton showers: The NLO case*, JHEP **04** (2013) 027, arXiv: 1207.5030 [hep-ph].

[37] H.-L. Lai et al., *New parton distributions for collider physics*, Phys. Rev. **D 82** (2010) 074024, arXiv: 1007.2241 [hep-ph].

[38] C. Borschensky et al.,
Squark and gluino production cross sections in pp collisions at $\sqrt{s}$ *= 13, 14, 33 and 100 TeV*, Eur. Phys. J. **C74**.12 (2014) 3174, arXiv: 1407.5066 [hep-ph].